



Universiteit
Leiden
The Netherlands

Scattering, loss, and gain of surface plasmons

Beijnum, F. van

Citation

Beijnum, F. van. (2013, May 15). *Scattering, loss, and gain of surface plasmons. Casimir PhD Series*. Retrieved from <https://hdl.handle.net/1887/20870>

Version: Not Applicable (or Unknown)

License: [Licence agreement concerning inclusion of doctoral thesis in the Institutional Repository of the University of Leiden](#)

Downloaded from: <https://hdl.handle.net/1887/20870>

Note: To cite this publication please use the final published version (if applicable).

Cover Page



Universiteit Leiden



The handle <http://hdl.handle.net/1887/20870> holds various files of this Leiden University dissertation.

Author: Beijnum, Frerik van

Title: Scattering, loss, and gain of surface plasmons

Issue Date: 2013-05-15

Transmission processes in random patterns of subwavelength holes

The optical transmission of random patterns of holes is believed to depend on the transmission of the independent holes only. By comparing the transmission spectra of random patterns with different hole densities, we show that the quasi-cylindrical wave plays an important role in the transmission of samples with a large hole densities. Furthermore we report on a speckle pattern seen in the transmission of these hole patterns. By studying the degree of depolarization in this speckle pattern, as a function of hole density, we are able to quantify the role of surface plasmons to the transmission.

F. van Beijnum, C. Rétif, C. B. Smiet, and M. P. van Exter, *Opt. Lett.* **36**, 3666 (2011).

3.1 Introduction

Research on the optical properties of holes in metal films has long been subject of fundamental and applied research. In 1944 Bethe calculated the transmission of a circular hole in a thin perfectly conducting film [55]. In 1998, the discovery of the extraordinary optical transmission of metal hole arrays [28] revived the interest in the optical properties of subwavelength holes and plasmonics. The ability of holes to couple light from free space to surface plasmons (SPP), makes them important for future applications [59, 60].

Calculating the transmission properties of subwavelength holes in metal films has proven to be a challenge [43]. The field at the metal surface turns out to be more complex than anticipated: not only SPP are excited at holes and slits, but also the quasi-cylindrical wave (CW) at a short distance from the hole, and the Norton wave at large distances [44–46].

So far, the transmission of random patterns of subwavelength holes were believed to accurately represent the transmission of a single hole [56, 61]. In this chapter we will argue that both the CW and SPP also contribute to the transmission of random patterns of subwavelength holes. To reveal these transmission processes we compare random patterns of different hole densities.

Figure 3.1a shows a scanning electron microscope (SEM) picture of a typical structure. We studied two sets of seven samples of which the inverse density (area per hole) is chosen qa_0^2 with $a_0 = 450$ nm and $q = 1, 2, 3, 4, 9, 16, 25$. One set has circular holes (average diameter: 120 ± 6 nm) and the other has square holes (average side length: 125 ± 5 nm). To avoid proximity effects in the fabrication the holes have a minimum side to side distance of 50 nm. Figure 3.1b illustrates the layer structure: a glass substrate with 150 nm gold, and 20 nm of chromium.

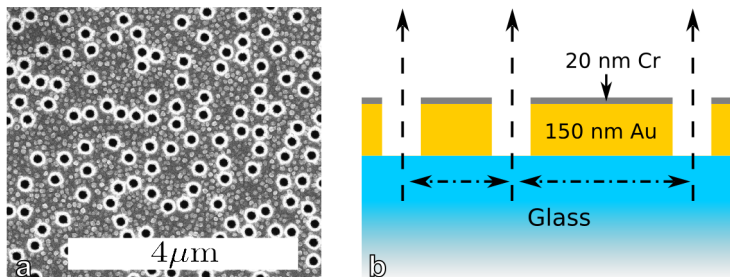


Figure 3.1: **a**, A SEM picture of one of the studied samples. The holes in a metal film are positioned randomly, samples with various hole densities are made. **b**, The layer structure of the metal film. The arrows illustrate direct (dashed) and indirect (dash-dotted) transmission processes that we study.

3.2 Modeling different transmission processes

Before presenting the experiments, we calculate the contributions of the transmission processes to the zeroth order transmission. We separate the transmission in a direct and an indirect contribution (see arrows Fig. 3.1b), and first include only SPP for the indirect transmission. We define $t_{d,i}$ to be the directly transmitted field for hole i , which is i -independent for identical holes. In the zeroth order the directly transmitted fields are all in phase, and therefore interfere constructively. The SPP field at hole i is a sum over the contributions from all neighboring holes j : $t_{s,i} = \sum_j t_{s,ij}$. As each indirect contribution $t_{s,ij}$ picks up a random phase, due to the random hole positioning, the amplitudes $t_{s,i}$ are uncorrelated. Hence the transmitted intensity T in the zeroth order diffraction is:

$$T = \left| \sum_{i=1}^N t_{d,i} + t_{s,i} \right|^2, \quad \lim_{k_{\text{spp}} \gg \alpha} \langle T \rangle = N^2 |t_d|^2 + N \langle |t_s|^2 \rangle, \quad (3.1)$$

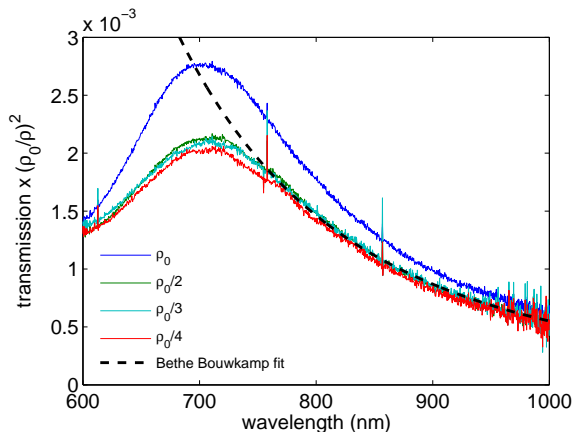
where $\langle \cdot \rangle$ denotes ensemble averaging, N is the number of holes, k_{spp} is the SPP wave vector and α is the inverse propagation length. In the limit $k_{\text{spp}} \gg \alpha$ there is effectively no correlation between amplitude and phase of $t_{s,i}$ and therefore the crossterms $t_{s,i} t_{s,j}^*$, $t_d t_{s,j}^*$, and $t_{s,i} t_d^*$ cancel out for $i \neq j$. In our experiments $N \gg 1$, making the SPP contribution negligible in the zeroth order.

In contrast to the SPP contribution just discussed, we expect the amplitude and phase of the CW to be correlated because this contribution decays rapidly, even within a wavelength. Hence the crossterms do not average out and an extra contribution proportional to N^2 is expected. However, this contribution will only be found if the average hole spacing is sufficiently small. Thus if we compare patterns with different hole density, the ratio $\langle T \rangle / N^2$ should change if the hole density is sufficiently large.

3.3 Recorded transmission spectra for different hole densities

We measure the zeroth order transmission of our samples using a standard white light transmission spectroscopy setup (not shown). The light from a halogen lamp is filtered (longpass, 600 nm) and coupled into a 200 μm fiber. The end facet of this fiber is imaged onto the sample with a magnification of 1.5. The transmitted light is imaged ($M=2/3$) onto a second fiber that leads to an Ocean Optics 2000+ USB spectrometer. The small NA ($\text{NA}=(6 \pm 2) \cdot 10^{-3}$) of the detection optics singles out the zeroth order transmission.

Figure 3.2: Intensity transmission of the four densest samples, normalized by $(\rho/\rho_0)^2$. The normalized transmission of the densest sample is enhanced as a result of the quasi-cylindrical wave.



To see an effect of the CW the transmission spectra are scaled with $(\rho_0/\rho)^2$, with $\rho_0 = 1/(0.45 \mu\text{m})^2$. For the low hole densities, the transmission of the structure approaches that of the gold itself ($T_{\text{gold}} \approx 3 \cdot 10^{-6}$). Hence, we need to correct for the transmission of the unperforated gold. Since both contributions are coherent we had to assume a phase relation to account for the interference, we choose the contributions to be in phase. This correction works for hole densities larger than $\rho_0/9$.

Figure 3.2 shows the scaled spectra for circular holes. The spectra for $\rho_0/2$, $\rho_0/3$, and $\rho_0/4$ overlap within 5%. In contrast, the scaled transmission of the densest sample at 685 nm is $37 \pm 1\%$ larger than that of the scaled transmission of the other three samples. This enhancement decreases gradually to $11 \pm 2\%$ at 600 nm, and to $18 \pm 5\%$ at 900 nm. For the square holes a similar but somewhat larger enhancement is found. We attribute the increase of the scaled transmission of the densest sample to the CW contribution discussed above.

Besides the hole density dependence of the spectra, the wavelength dependence of the transmission has attracted much interest too [55, 56, 62]. The long wavelength tail of the transmission can be fitted using the Bethe-Bouwkamp formula [55, 63], (see e.g. [43]). The fit results in a diameter of 130 nm, which is surprisingly close to the diameter of 120 ± 6 nm measured in the SEM pictures.

A remaining issue is whether the maximum in the transmission is a shape resonance. The transmission maximum appears to be dependent on the hole size, since transmission maxima of the (larger) square holes are at a larger wavelength (750 nm). In calculations and experiments on perfect electric conductor films such a size dependent transmission maximum is found too [43, 62, 64, 65]. In ref. [43] it is shown that a maximum is expected at

$kr \approx 1.6$ for zero thickness and at $kr \approx 2.1$ for a thickness equal to the radius. However, in our experiments a maximum is found at $kr = 0.8$, hence the origin of this feature is not yet resolved.

3.4 Polarization analysis of far field speckle pattern

We not only observe the zeroth order diffraction peak, but also a speckle pattern (order 10^{-3} , see Fig. 3.3a). If we illuminate the sample with polarized laser light, and place an analyzing polarizer, we see that the zeroth order can be suppressed while the speckle pattern remains visible (see Fig. 3.3 b). The speckle pattern intensity for the orthogonal polarization is roughly an order of magnitude smaller than that of the parallel polarization. Moreover the pattern has changed (only 2% correlation in speckle patterns). To the best of our knowledge, this speckle pattern has never been reported.

Before analyzing the speckle patterns in further detail, we calculate the contributions to the speckle intensity at an angle $\vec{\theta}$. In contrast to the analysis of the zeroth order, the contributions of the direct transmission will not be in phase. Two holes at position \vec{r}_i and \vec{r}_j will have a phase difference $k_{\parallel}(\vec{r}_i - \vec{r}_j)$. Hence, the transmitted intensity in the speckle pattern is:

$$\langle T(\theta) \rangle = N \left(|t_d|^2 + \langle |t_s|^2 \rangle \right). \quad (3.2)$$

In contrast to the zeroth order transmission, both contributions are now incoherent and therefore both scale with N . However, one would expect that the direct contribution only has the incident polarization, whereas the SPP contribution is partially depolarized.

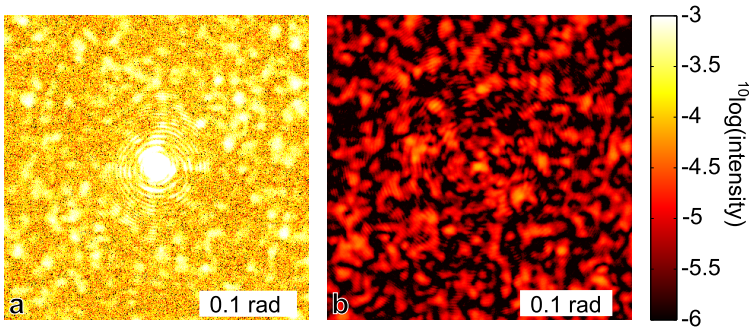


Figure 3.3: Angular transmission pattern of the sample of with $\rho/\rho_0 = 16$ illuminated with a weakly focussed beam. **a**, Using an analyzing polarizer parallel to the incident polarization, we see a zeroth order diffraction peak and a speckle pattern. **b**, By rotating the polarizer 90° the zeroth order is suppressed. All intensities are normalized to the maximum intensity of the zeroth order in **a**.

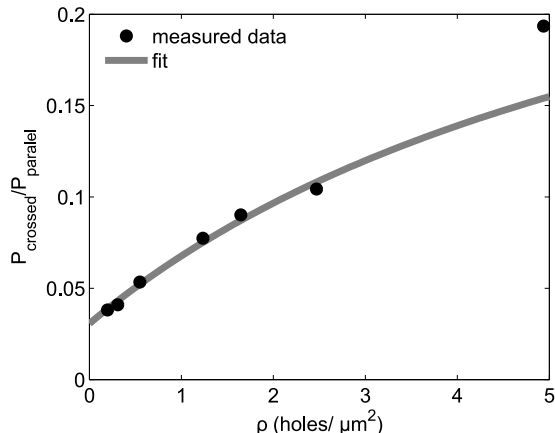


Figure 3.4: The ratio of the power in the speckle pattern for parallel over the orthogonal polarization. The ratio increases with hole density, showing that there is an indirect contribution.

Using a simple model we calculate the SPP contribution at hole i from all other holes j using: $t_{s,i} = \sum_j t_{s,ij}$. We assume that the light propagates along a straight line from hole j to i . The field will be damped due to absorption and light that is scattered out of the surface plasmon mode, making $t_{s,ij} = (C(\phi)/\sqrt{r_{ij}}) \exp((\alpha + ik_{spp})r_{ij})$. The excitation efficiency $C(\phi)$ is a function of the angle ϕ between the incident polarization and the propagation direction, and has unit $\sqrt{\text{m}}$. The loss rate due to scattering is denoted as α .

The exact form of $C(\phi)$ is unknown, but we can approximate it using a projection argument: $C(\phi) \propto \cos \phi$. Besides the excitation efficiency, there is a detection efficiency. Using a polarizer parallel or orthogonal to the incident polarization, this results in an extra factor of $\cos \phi$ or $\sin \phi$ respectively. Hence, the fraction of the average power in the surface modes for the parallel polarization ($C_{\parallel}^2 \propto \langle \cos^4 \phi \rangle$) is three times larger than in the orthogonal polarization ($C_{\perp}^2 \propto \langle \cos^2 \phi \sin^2 \phi \rangle$). The ratio between the power in the speckle pattern for the parallel and orthogonal polarization is thus:

$$\frac{P_{\perp}}{P_{\parallel}} = \frac{|t_{d,\perp}|^2 + \rho C_{\perp}^2/(2\alpha)}{|t_{d,\parallel}|^2 + \rho 3C_{\perp}^2/(2\alpha)}, \quad (3.3)$$

where $|t_{d,\perp}|^2$ is the depolarized part of the direct transmission. Thus at low hole densities, one measures the depolarization due to imperfections of the holes. As the hole density increases the relative amount of depolarized light will increase, due to the increased outcoupling of SPP.

For all seven samples we measured the ratio between the power in the speckle pattern for the parallel and orthogonal polarization. In Fig. 3.4 this ratio is plotted versus the hole density. The measured ratios increase with hole

density from 0.03 to 0.2. The fact that the depolarization is density dependent proves the existence of an indirect contribution. When fitting the data to the theory (line in Fig. 3.4), we see that the data point at the largest hole density can not be fitted properly. However we expect the CW to contribute to both the zeroth order and the speckle pattern, because the CW contribution is random but with a correlation between amplitude and phase.

From the fit we conclude that $C_{\parallel}^2/(2\alpha |t_{a,\parallel}|^2) = 0.14 \pm 0.02 \mu\text{m}^2$. This means that for a hole density of $1 \mu\text{m}^{-2}$ and parallel polarizers the SPP contribution is 14% of the direct transmission. From the fit we find: $|t_{a,\perp}|^2 = 0.031 \pm 0.005$, meaning that 3% of the directly transmitted light is depolarized by the holes. By imaging a low density sample, we observe that the transmission through individual holes can be blocked within experimental accuracy using a polarizer. However the blocking angle varies from hole to hole, ranging from -10° to 10° , which in rough agreement with the 3% found in Fig. 3.4.

3.5 Conclusion

We have shown that random patterns of subwavelength holes of variable hole densities are an ideal tool to unravel transmission processes. In the zeroth order transmission the direct transmission and quasi-cylindrical wave (CW) are the only relevant contributions. By analyzing a newly reported speckle pattern for different polarization states, we have quantified the SPP contribution to the transmission.

In future work the enhancement as a result of the CW can possibly be predicted using a recent theoretical calculation of the CW contribution near a single hole [46]. Moreover, the analysis of the speckle pattern could be done for different materials or wavelength ranges, to study the importance of the SPP and the CW there.

